Journal Name

ARTICLE

General aspects in the use of graphenes in catalysis

Sergio Navalón[a,*] José Raúl Herance,[b] Mercedes Álvaro,[a] Hermenegildo García[a,c,d,*]

Received 00th January 20xx,
Accepted 00th January 20xx

DOI: 10.1039/x0xx00000x

www.rsc.org/

This perspective is aimed at presenting some issues that, in our opinion, have still to be better addressed in the field of graphenes as catalysts. After an introductory section, the article comments on how the number of layers present on the catalyst, termed frequently as graphene, could be in some cases in contradiction with good practices about what should be or not considered as graphene. It will also be commented that some of the characterization tools that are employed in some cases for graphenes as catalysts, like specific surface area measurements based on isothermal gas adsorption on powders or XRD patterns are not well suited to characterize graphenes. The potential role of impurities and structural defects on graphene catalysis has been highlighted showing the importance of providing exhaustive analysis of the materials. The perspective includes a final section with our view on future progress and wider consensus in the use of graphene in catalysis.

Index

1. Introduction

Catalysis in the XXth Century was dominated by transition metals, frequently noble or critical elements.[1-5] For the sake of sustainability, one of the current research lines in catalysis is to find replacements for scarce and precious metals by developing alternative catalysts based on abundant and sustainable elements.[6-8] This area has flourished in recent years due to the expansion of carbocatalysis employing carbon allotropes as metal-free catalysts.[8-16] These carbon materials can also be used as supports on which other particles imparting the catalytic activity are deposited.[17] Among the various carbon allotropes, graphene and related materials are currently attracting much attention, there being several reasons to explaining this choice, including multigram availability, well-defined structure, ease of characterization and the possibility to alter their chemical composition, among other ones.[18-22] From the catalysis point of view, the large specific surface area of graphene that is even larger than most of active carbons, together with the easy dispersability in liquid solvents, making unnecessary mass transfer among liquid-solid phases, represent also considerable advantages respect to other carbon materials.[13]

The relative novelty of the use of graphene in catalysis has led in some cases to use conventional characterization techniques very useful in the case of tridimensional, porous and non-porous solids also for graphenes, while other necessary information specific for atomically thick bidimensional (2D) materials has sometimes been neglected. The present perspective is aimed at showing how the specific features of graphene, such as its single layer configuration, have not been in some cases adequately considered and an inappropriate use of the term graphene has been used for some bulk, powdered materials, where independent single layer sheets are not present.

Besides the number of layers, the porosity and XRD pattern of graphene materials have been in some cases given as a way to characterize these materials, whose 2D morphology and single atom thickness are not suitable to be characterized by these textural or crystallographic techniques. An important issue in the case of some graphene samples is the presence of metal or amorphous carbon impurities that could be responsible for a large proportion of the observed catalytic activity. This raises the issue of providing convincing analytical

[a.] *Departamento de Química, Universidad Politécnica de Valencia, Camino de Vera, s/n, 46022 Valencia, Spain.*
[b.] *Molecular Biology and Biochemistry Research Center for Nanomedicine Vall d'Hebron Research Institute (VHIR), CIBBIM-Nanomedicine, CIBER-BBN Passeig de la Vall d'Hebron 119–129, 08035 Barcelona (Spain).*
[c.] *Instituto de Tecnología Química CSIC-UPV, Universidad Politécnica de Valencia, Av. de los Naranjos s/n, 46022 Valencia, Spain.*
[d.] *Center of Excellence for Advanced Materials Research, King Abdulaziz University, Jeddah, Saudi Arabia.*

data of the graphene samples used in catalysis and to make controls on the possible role of the impurities at the low concentrations possibly present in graphene.

Related to the previous point, there is ample evidence showing that ideal, perfect graphene has not catalytic activity for different reaction types, like aerobic oxidations and reductions,[12, 13] for which defective graphenes are active. The point of the role of defects on the catalytic activity and, more generally, the nature of the active sites on carbocatalysts is a very important issue that deserves to be studied in detail, because it could serve to determine the intrinsic activity of these sites and to devise synthetic procedures to increase their density on graphene materials.[12]

Thus, the purpose of the present perspective is to comment on good practices that could serve to clarify some of the open issues that could arise when using graphenes to promote chemical reactions, particularly for their use as metal-free catalysts. Although graphene and related materials have been widely used as electrocatalysts[23-25] and photocatalysts[25-27] and there is also abundant literature on these applications in the present review we have limited ourselves to the case of the use of graphenes in catalysis.[12, 13, 28] The last section of this article provides our view on the current status of the use of graphene in catalysis and which should be in our opinion the future developments in the field to exploit the distinctive features and properties offered by graphene in catalysis.

2. Single or few-layers graphenes in catalysis

Graphene is defined as a single layer of one atom thick sp^2 carbon atoms in hexagonal arrangement.[29, 30] Graphite is constituted by the stacking of multitude of well-aligned, parallel graphene layers with high crystallinity (Figure 1). In an editorial, the journal Carbon has remind the appropriated nomenclature for 2D carbon materials related with graphene.[29] According to these recommendations, attention should be paid to the number of layers that constitutes 2D carbon materials and the term graphene should be exclusively used for an isolated single layer building block. The term graphene layer should be employed when referring to the individual component in the structure of graphite and other 3D carbons. It should be indicated that the material is few- or multilayer graphene when there is more than a single layer.

One controversial and important issue in the nomenclature of graphene and related materials is the maximum number of layers to denote still these materials to be considered as belonging to the graphene family, even though as multilayer.[29] For example, using top-down exfoliation strategies from graphite or turbostratic carbons (Figure 1), the resulting number of exfoliated graphene layers can be one single layer (graphene; 0.34 nm thickness) or platelets of stacked graphene layers up to tens of nanometers. In this sense, it is known that the electronic structure of multilayer graphenes becomes indistinguishable from graphite when the number of layers exceeds ten.[30]

Related to the previous issue of multilayer graphenes and their thickness, the use of the term "nanomaterial" for

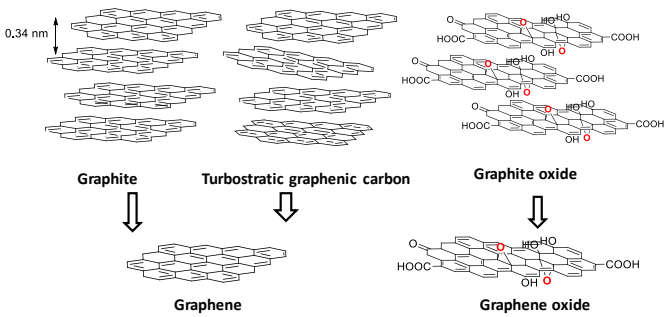

graphene is not recommended, since the definition of graphene already implies the subnanometric thickness, the limit in thickness for multilayer graphene being below 10 nm. For deeper detail, the nomenclature of bilayer- or trilayer-graphene can be employed for materials with 2 or 3 countable stacked graphene layers. The term few-layer graphene is recommended when the number of graphene layers is from 2

Figure 1. Pictorial illustration of the structure of graphite, turbostratic carbon and graphene-based materials and their exfoliation to afford graphene related materials.

to about 5. Multilayer graphene can be employed when the number of graphene layers is between 2 and about 10. It is, however, very frequently in the area of carbocatalysis that, due to the conditions required to carry out the reaction and the presence of reagents and substrates, no attention is paid to the number of layers of the graphene employed in the process, even though, this is an important issue that could exhibit a profound influence on the activity of the material.[13, 16]

On the other hand, the nomenclature of the graphene family is not only a function of the number of the stacked graphene layers, but also depends on the lateral dimensions of the sheet (Figure 2). Thus, the terms graphene nanosheet or microsheets should correspond to a single-atom thick sheet of hexagonally arranged, sp^2-bonded carbon atoms with lateral dimensions below 100 nm or between 1 and 100 μm, respectively.[29] If graphene has lateral dimensions smaller than 10 nm the material should be named as graphene quantum dot.

In the context of the use of graphene and related materials in catalysis, either as metal-free carbocatalyst8-16 or as support of active components,[17, 31] the above recommendations regarding good nomenclature practices are frequently ignored, resulting often in ambiguity and confusion

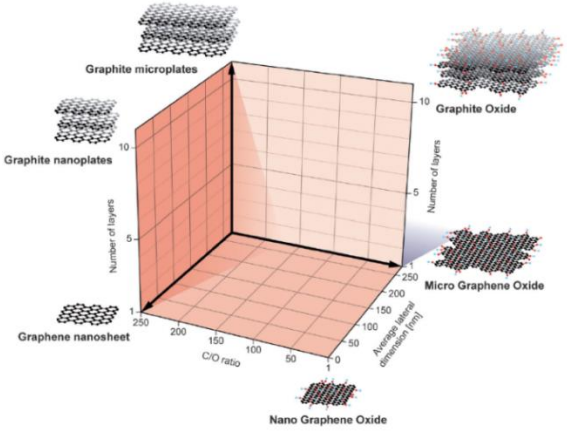

Figure 2. Classification grid for the categorization of different graphene types according to three properties: number of layers, average lateral dimension, and atomic carbon/oxygen ratio. The different materials drawn at six of the corners represent ideal materials.[32]

about the material being use as catalyst. Thus, for instance, according to the recommended definition, the term graphene should only be used when the graphene material is present as a film on a substrate surface or in dispersion in a liquid medium. In other situations, particularly for powders, the term graphene to denote the catalyst could be misleading. Thus, one general case in where single layers of G may not be present is when using powders as catalysts as for instance in reactions in gas phase.[33-35] In the case of powders, even if they are amorphous, stacking of the constitutive G layers should be present in different regions of the material and the single layer morphology could not be claimed in the powder in most of the cases. If, however, the powder possesses any kind of sponge-like structuring preserving the single layer configuration of the walls, then, the term of graphene catalyst can be applicable even for gas phase reactions.[36] In fact these materials are highly promising as adsorbents of gases[37, 38] and for various applications in energy, particularly for Li-air batteries[37, 39] and supercapacitors.[40-42]

3. Porosity and X-ray diffraction of graphene

Related to the previous comment respect to the single layer morphology of the carbonaceous material under catalytic conditions, this are certain characterization data of graphenes that have been frequently reported and that could be in contradiction with the single layer morphology.

One of these properties is porosity and the presence of micro- or mesopores in the material.[43] Porosity, characterized by both pore size distribution and pore volume, is a relevant property having strong influence on the catalytic activity in many solids that have a 3D morphology such as zeolites,[44, 45] metal-organic frameworks,[46] porous silicas,[47] porous aluminophosphates,[48] etc. In these cases, the 3D morphology of the solid particle makes possible the existence of channels and cavities inside the crystal that could be open to the external surface, allowing mass transfer from the exterior to the interior of the particle. Even more, when the material is crystalline the pore size can exhibit a very narrow size distribution, either in the region of micropores (below 2 nm), or in the meso- (2-50 nm) and macropore (over 50 nm) range. However, it is obvious that 2D sheets of single layer configuration cannot possess this type of structural features and, therefore, there is not point on providing the porosity of Gs, particularly when these materials are going to be used later as fully dispersed catalysts. Porosity in powdered samples containing graphenes refer to the way in which the layers stack and are not relevant when they are going to be redispersed to become single or few-layers graphene.

In one review covering the use of porous graphene this type of materials has been defined as a collection of graphene-related materials on the basal plane.[49] In this context, to avoid confusion with 3D nanopores materials it would be preferable to refer to the presence of these defects as holes in graphene or, at least, 2D nanopores.

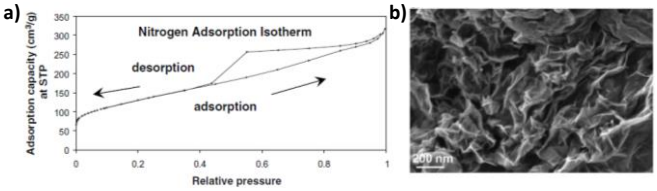

Figure 3. a) A SEM image of aggregated rGO powders; b) Nitrogen adsorption and desorption isotherms for rGO powders.

For instance, it has been reported that chemical reduction of GO by hydrazine may result in the formation of reduced graphene oxide (rGO) samples whose powders constituted by the stacking of several defective graphene sheets exhibit a high surface area of BET 436 $m^2 g^{-1}$ measured by isothermal N_2 adsorption (Figure 3a).[50] Scanning electron microscopy (SEM) images, however, clearly show agglomeration of GO during the transformation to rGO (Figure 3b).[50] It was indicated that the shape of the isotherm indicates that the material contains both micro and mesopores, but, of course, these pores refer to the powdered material and not to exfoliated rGO. It should be noted that the common technique to determine porosity is based on isothermal gas adsorption on powders and these measurements cannot be extrapolated to the case of exfoliated rGO.[11]

More recently a family of 3D graphene nanoarchitectures have appeared and in those cases the term porosity can correctly by applied to these graphene sponges. For instance Ruoff and co-workers reported that KOH treatment of GO can lead to high surface area (over 3100 $m^2 g^{-1}$ BET) highly porous 3D-materials due to the formation of covalent bonds between the initially independent sheets.[42] Certainly 3D graphene derived carbons are very interesting materials with applications as supercapacitors and electrodes but they have a different morphology from 2D independent sheets.[40, 51] Analogously, a series of 3D porous graphene materials have been prepared by pillaring graphene layers with for example, rigid organic molecules such 1,4-ethynyl substituted benzenes (Figure 4a).[52] For these pillared graphenes a pore distribution from micro to meso range (1 to 3 nm) and pore volume of 0.74 $cm^3 g^{-1}$ have been estimated by isothermal gas adsorption measurements. Other examples have prepared 3D graphene-based powdered materials from sucrose and GO, resulting in a material with graphene walls without any possibility to stack that exhibit specific surface areas as high as 3,523 $m^2 g^{-1}$ close to theoretical values and mesoporosity (Figure 4b).[53]

Closely related to the previous comments on porosity, common misconception in the use of graphene as heterogeneous catalyst is to determine surface area by isothermal N_2 adsorption on evacuated powders. As commented earlier the use of powders in this measurement

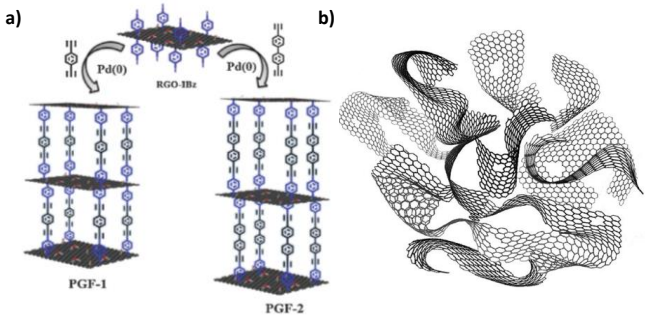

Figure 4. a) Illustration of the preparation of pillared porous graphene frameworks. [52] b) Proposed 3D model structure of a disordered porous 3D graphene material.[53]

does not really correspond to the state of the fully exfoliated material that will be later achieved by suspending the powder in a liquid medium by extensive sonication or other exfoliation procedure. When using powders for surface area measurements unavoidable stacking, particularly after evacuation of adsorbed molecules necessary to perform the measurement, should occur. Not surprisingly values of specific surface area for graphene powders or graphene oxide materials as low as a few $m^2\ g^{-1}$ and in the large majority of the cases below 100 $m^2\ g^{-1}$ have been reported.13 These specific surface area values are much below the theoretical surface area of ideal G that has been estimated about 2650 $m^2\ g^{-1}$ [21] and only reflect the inadequacy of isothermal gas adsorption on powders to determine surface area in suspensions or films.[13]

In this regard, Aksay and others have developed alternative methods to determine surface area of graphene-based materials directly in suspension.[54] The methods are based on the adsorption ability of graphenes for polycyclic aromatics forming strong association complexes and this adsorption can be conveniently followed by different analytical techniques. In the case of polycyclic dyes, such as methylene blue, adsorption can be followed by colorimetry monitoring the free dye concentration in solution.[55] The calculations determine the number of molecules adsorbed on a given weight of the material and the surface occupied by one adsorbed molecule. As in the case of isothermal gas adsorption, a basic assumption on these measurements is that full monolayer coverage of the dye on graphene can be determined somehow. The case of methylene blue is particularly appropriate for GO because this dye is a cationic compound that strongly associates negatively charged graphene oxide (Figure 5a).[55] In this case, absorption

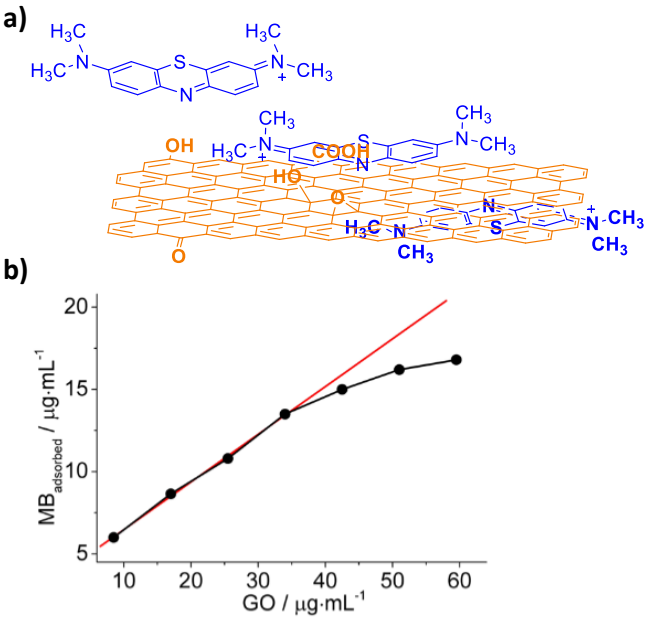

Figure 5. a) Formation of strong conjugates between methylene blue and GO and G materials due to Coulombic attractive forces and π-π stacking; b) Plot of the amount of MB necessary to reach the maximum intensity of the 580 nm band characteristic of methylene blue-GO conjugate and formation of precipitate vs the concentration of GO. The straight line corresponds to an extrapolation for the best fitting of the more diluted data points, showing a gradual deviation of the experimental data points from the linearity reflecting an increasing aggregation of GO as its concentration in aqueous solution increases.[55]

spectroscopy detects the formation of two distinctive adsorbates that have been assigned to isolated adsorbed methylene blue and adsorbed methylene blue forming aggregates (Figure 5b). Even more, when the surface of GO is believed to be fully covered by GO, precipitation of the methylene blue-GO conjugate from the aqueous suspension is observed, making even easier the determination of the amount of adsorbed dye remaining in the clear solution. This type of measurements have revealed much larger surface areas, well above 1,000 $m^2\ g^{-1}$, for dispersions of GOs for which surface area measurements based on isothermal gas adsorption in powders have given values below 80 $m^2\ g^{-1}$. Furthermore comparison of the theoretical and experimental surface area can give an indication of the degree of exfoliation of the suspended graphene sample and, in some cases, it has been found that over 80 % of the total weight being present on the suspension should be as single layer. Moreover, this level of exfoliation has been found to decrease upon increasing the concentration of the suspended graphene material, suggesting that high exfoliation degrees can only achieved for very diluted dispersions (below 0.1 mg mL^{-1}) and that an increase in the concentration necessarily causes gradual graphene aggregation.

These types of measurements can be complemented with atomic force microscopy (AFM) characterization of the nanometric vertical high of the platelets obtained by depositing a drop of the suspension on atomically flat surfaces

such as those of crystalline silicon wafers or mica.[22] However, to be meaningful the AFM study has to determine the vertical high of a statistically relevant number of graphene particles in the material to determine the thickness distribution of the sheets present in suspension. In the case of few-layers graphene other techniques such as light absorption at high wavelengths typically 650 nm,[56] and deposition and shape of the 2D-band in Raman[57] can also be used to have an indirect estimation of this parameter.

In the case of preparation of rGO from well exfoliated GO, it has been found that the nature of the reducing agent to transform GO to rGO can affect not only to the reduction degree of the sheet, but also to the exfoliation of the resulting graphene layers.[58, 59] For example, it has been reported that thermal reduction at 1000 ºC or chemical reduction by hydrazine of GO are more adequate to obtain a high degree of exfoliation in the resulting rGO compared to the use of $NaBH_4$ as reducing agent that forms stacked G sheets (Figure 6).[58]

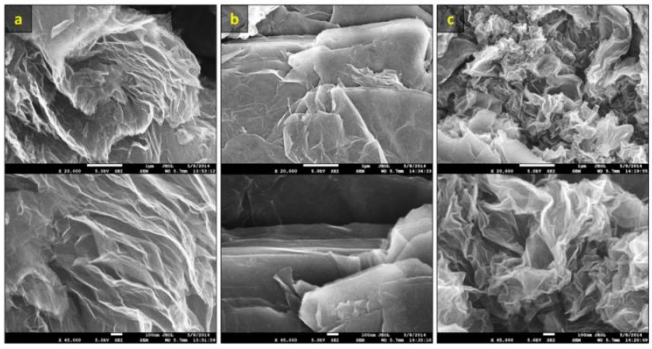

Figure 6. SEM images of (a) rGO samples obtained by Hummers oxidation followed by thermal reduction, (b) rGO formed by Hummers oxidation followed by $NaBH_4$ reduction and (c) Hummers oxidation and hydrazine reduction.[58]

In this regard, other reports have stablished the higher electrical conductivity of rGO films when using $NaBH_4$ as reducing agent respect to the use of hydrazine.[60] The lower electrical conductivity of the rGO when using hydrazine can be due to the partial functionalization of rGO with C-N groups that would act as electron donors, compensating the hole carriers in the resulting material and decreasing the electrical conductivity.

Similarly to the previously commented inadequate surface area and porosity measurements, another conventional technique that is frequently misused for graphene characterization is XRD. Bulk graphite being a crystalline solid constituted by the stacking of graphene layers was among the first solids to be studied by X-ray diffraction by Bragg in the early stages of the development of X-ray diffraction techniques at the beginning of the XXth Century.[61] When graphite (Figure 7a) is deeply oxidized by the Hummers oxidation method or by alternative procedures the XRD of graphite changes reflecting the expansion of the interlayer distance in graphite oxide that is now constituted by graphene oxide layers (Figure 7b).[62, 63] Reduction of GO to rGO may lead to some stacking of rGO sheets and powdered samples can be also monitored by XRD (Figure 7c). However, when dealing with single layered materials, like fully exfoliated graphene or GO, no X-ray diffraction pattern should be observed for these samples. Accordingly, those reports presenting XRD of graphenic materials are really reporting solids in where stacking with higher or lower crystallinity degree, depending on the width and position of the diffraction peaks is occurring. In other words, XRD is not applicable to the study of single layer graphene or GO.

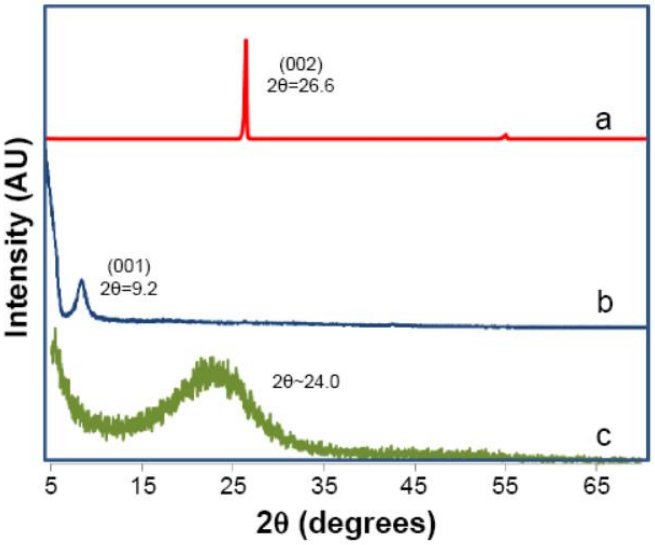

Figure 7. XRD patterns of (a) graphite and those reported for (b) GO and (c) rGO powders.[62]

4. Ideal versus defective graphene

As it will be commented below the most interesting graphene type from the point of view of their activity as carbocatalysts is defective graphenes.[12, 13, 64] Sometimes defects on graphenes are introduced unintentionally, but, however, the resulting electronic and chemical properties of the graphene sheet can be modified as consequence of the presence of these defects.[65-68] These defects can have a large impact in the observed catalytic activity.[12] In this regard, Raman spectroscopy is a very appropriate technique to monitor the presence of defects by observation of the D band around 1,350 cm^{-1} that is associated with the presence of sp^3 carbons and carbons in defective sites (Figure 8a).[57] Therefore, it can be assumed that those graphenes having interesting catalytic properties should be those presenting a relatively intense D band. Moreover, the relative intensity of the characteristic graphitic G peak at about 1,580 cm^{-1} vs the intensity of the D peak (I_D/I_G) can provide a quantitative measurement of the density of defects on the defective graphene. Some examples have found a positive relationship between the I_D/I_G ratio in various thermally annealed rGO and the increase in the catalytic activity for peroxymonosulfate activation.[69]

In addition, Raman spectra can inform about the single or few layer configuration of graphene film by determining the position and shape of the 2D band, typically appearing about 2,700 cm^{-1}. Single layer graphene films should present narrow and sharp 2D peak at lower Raman frequencies compared to few layers or multilayers graphene films (Figure 8a).[57]

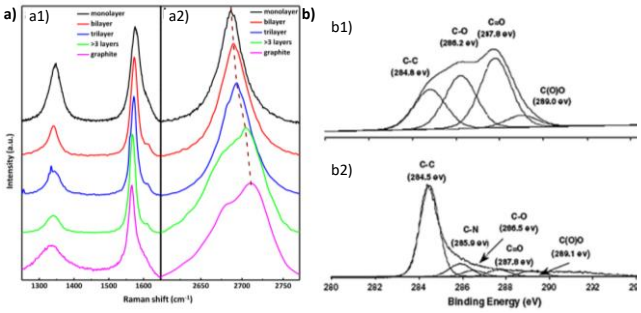

Figure 8. a) Evolution of the Raman spectra with increasing number of layers. In (a1) the D band is positioned at 1347 cm^{-1} and the G band is positioned at 1578 cm^{-1}, without any considerable change with increase in the number of layers. In (a2) the 2D band position undergoes a blue shift from 2686 cm^{-1} for graphene to 2703 cm^{-1} for multi-layer graphene along with an increase in the full width at half height from 32 to 64 cm^{-1}. The features corresponding to graphite are also included for comparison.[57] XPS peaks: b) C1s of GO (b1) and hydrazine-reduced GO (b2).[50]

The presence of defects that could be associated with sites exhibiting catalytic activity can also be determined by XPS.[12] First, the presence of other elements than carbon (Figure 8b), particularly oxygen, but also nitrogen and sulfur, is frequently detected in the XPS measurements of defective graphenes. In the second place, the shape and binding energy of the C1s peak in high resolution XPS becomes less symmetric and broader, expanding a range of binding energies that reflects the presence of carbon atoms with different types of coordination environments. Quantitative XPS measurements in powders can provide an atomic ratio of the different elements that, however, may not necessarily correspond to the bulk composition of the material. This mismatch is due to the fact that while combustion chemical analysis determines the percentage of an element in the bulk material, XPS is only probing the composition of a very thin layer of the surface of the material. Only in the case that XPS is monitoring films of single layer or few layers graphenes for which all the film is probed by the soft X rays used in this technique, this elemental composition by XPS can really correspond to the material.

As commented earlier, the strict definition of graphene does not contemplate the presence of defects on the sheet that has to be constituted exclusively by carbon atoms in hexagonal geometry.[29, 30] However, it is increasingly recognized that the catalytic activity of graphenes derives from the presence of defects in the structure.[12, 64] These defects can be Stone-Wales defects formed by rotating a carbon-carbon bond 90 º (Figure 9A), carbon vacancies or holes on the interior of the sheets (Figure 9B) or the presence of heteroatoms, such as oxygen, nitrogen, boron, sulfur and others, covalently bonded to carbon.[12, 16, 63, 64] Also the periphery of the graphene sheet (Figure 9C) should be considered as defect and can act as active site in catalysis. Peripheral carbon atoms can become increasingly important when the sample is constituted by small-size graphene sheets, well-below the typical micrometer size that is common for many graphene samples, particularly those obtained from graphite flakes.[12] Also, the catalytic activity of carbon nanoribbons formed by zipping CNTs arises from the atoms at the periphery of the ribbons.14 Although the issue of whether or not these defective materials should be considered as graphenes or not may arise, the simplest convenient approach is to denote these materials as defective graphenes.

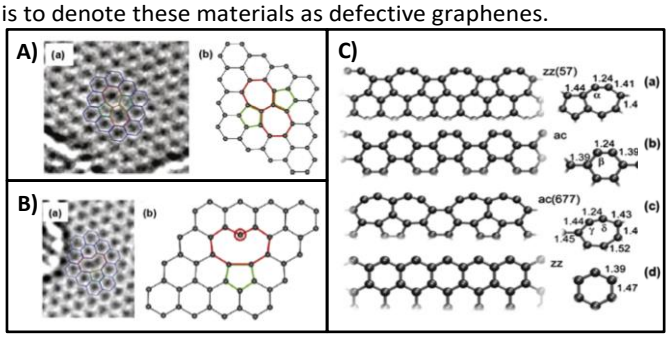

Figure 9. A) Experimental (a) and DFT model (b) of Stone-Wales defect (577); B) Experimental (a) and DFT model (b) of a single carbon vacancy V1(5-9); C) Different edge reconstructions in graphene: (a) reconstructed zigzag; (b) armchair edge; (c) (677) reconstructed armchair edge; (d) zigzag edge. The numbers in brackets indicate the size of the rings at the defect site.

One particular case of defective graphene with reported catalytic activity is the material obtained from GO by reduction either chemically or by physical treatments.[63] An important feature of rGO is that it contains some residual oxygen that is present as carbonyl groups and carboxylic acids as well as hydroxyls and ethers. While the oxygen content of GO is above 40 wt% and in some cases close to 60 wt%, reduction of this material resulting in rGO decreases considerably the oxygen percentage to values that are about 10 wt%. These residual oxygenated functional groups do, however, play an important role in the catalysis because they can act as catalytic centers. Also, during the reduction of GO evolution of CO_2 and CO can create carbon vacancies and holes that are present in the resulting rGO.

Heteroatoms present on graphene can act as active sites in different catalytic reactions.[70] Nitrogen is the most widely studied heteroatom in doped graphenes.[12, 71] There are several ways in which nitrogen atoms can be introduced as dopant element, including chemical vapor deposition of gaseous nitrogenated organic compounds on hot metal surfaces.[13] This procedure may have the advantage that composition of the graphene can be controlled by the composition of the gas present in the CVD chamber. However,

this preparation procedure requires dedicated specific equipment for the preparation of graphene and produces only graphene films that are not the most employ form of graphene on catalysis.

An alternative doping procedure that is more convenient for the preparation of larger quantities of nitrogen-doped graphene without the need of special equipment is the reduction of GO under hydrothermal conditions using aqueous ammonia solutions or even hydrazine.[13] In this process nucleophilic addition of the nitrogen reagent on the GO forms covalent C-N bonds that upon further reduction and partial reconstitution of the graphene sheet results in the presence of certain nitrogen content on the rGO. XPS analysis of this N-containing rGO reveals the presence of several types of N atoms including those denoted as quaternary, pyridine-like or pyrrolic nitrogen atoms.[13] By preparing a set of samples with different proportion of these types of nitrogen atoms, conclusions on which is the more adequate nitrogen type to act as active site can be deduced. However, the problem of this approach is that together with nitrogen, a variable proportion of oxygen is also present in N-doped rGO. Varying the conditions to modify the N atom distribution leads also unavoidably to a variation of the oxygen content and nature of the oxygen functional groups. However, most of the studies in this area have not paid attention to the presence of oxygen and the change in its content and distribution from sample to sample. Most of these studies have attributed exclusively the catalytic activity of the resulting rGO samples to the nitrogen atoms, disregarding any possible contribution or synergism due to oxygen.[12] It should be commented that oxygenated functional groups are also well-known active sites for many reactions in the absence of any nitrogen content and properties like acidity and redox activity have been found to depend on oxygen functional groups.[12, 13, 16]

Besides nitrogen, there are many other reports in the literature[70, 72, 73], showing that graphene doping by other heteroatom such as B, P or S and co-doping of more than one heteroatom, also introduce active sites[12] to promote different reactions including peroxide decomposition, generation of hydroxyl radicals from H_2O_2, hydrogenations, aerobic oxidations among others.[12, 13, 70]

5. Impurities in graphene

In a series of papers, the different impurities present on graphene as consequence of the preparation procedure have been reported.[12, 13, 50, 74-82] Frequently, these impurities are metals, carbonaceous debris, functional groups as well as surfactants, among other possible unwanted elements (Figure 10). In the following sections, the impact of these impurities on graphene in its catalytic activity will be commented.

5.1. Metal impurities

In the field of homogeneous or heterogeneous catalysis it is well-established that the presence of several transition metals such as Cu, Ni or Pd even at trace levels, can act as Lewis or redox centers in many catalytic reactions.[83-86] Furthermore, the presence of apparently inert alkaline metals, such as K^+, can alter the electronic properties of Gs and, therefore, could modify the behavior of the graphene-based material when employed as catalyst, photo- or electrocatalyst.[87-90] Therefore, kinetic tests should firmly establish if the graphene materials are really active as metal-free catalysts or metal impurities are playing this role. This situation is similar to that of CNTs when employed as carbocatalysts, photocatalysts and electrocatalysts, where many reports have highlighted that the presence of metal impurities is responsible for the observed catalytic activity.[91-97] Typically, metal impurities of CNTs are introduced during their preparation,[98-102] even harsh purification procedures are not completely efficient to remove these impurities.[103, 104]

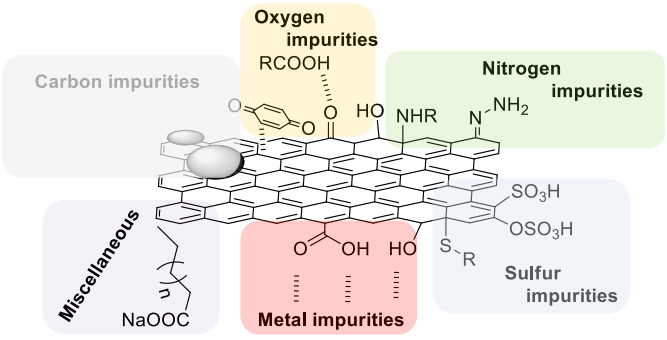

Figure 10. Illustration of some common graphene impurities.

Graphite is a natural mineral that frequently contains in its composition a variety of metals as impurities (Table 1).[90, 105, 106] Consequently, one can assume that graphene obtained from natural graphite contains metal traces. Therefore, metal impurity determination is mandatory in order to study the possible impact of their presence in the resulting catalytic activity. Several techniques can be used for metal trace determination in graphite or graphene-based materials, while the detection or quantification limits varies from one to other and this fact should be kept in mind. Determination of metal impurities at trace levels requires the use of analytical or spectroscopic techniques such as ICP-MS/OAES,[107] neutron activation analysis[61] and/or X-ray fluorescence (ppm).[107] EPR and dc magnetic susceptibility measurements have been highlighted as ultrasensitive methods for metal impurity determination in CNTs.[108] XPS technique is frequently employed for this purpose although has a general detection

Table 1: Metallic impurities content (ppm) in graphite determined by ICP-MS analytical technique.

Fe	Ni	Mn	Mo	Co	Ref.
240	190	-	4.7	0.37	90a
4224	33.7	24.9	-	3.3	105
55.2	2.9	-	0.45	0.03	106

[a] 7.2 ppm of Cu was also found

limit for some metals of 0.1 wt% (1000 ppm).[108, 109] In addition, XPS measurements are limited to surface analysis (less than 5 nm depth) and it could happen that some impurities present in stacked graphene layers may not be detected by XPS or not quantified accurately.[107, 108] Although EDX has allowed determination of the presence of electrocatalytically active iron metal impurities in graphene screen-printed electrodes,[110] other studies have reported that EDX detector can provide false-negative results, when employed for determination of trace levels of metal nanoparticles intercalated in CNTs.[108]

One important point to be considered in GO and rGO is the presence of metal and non-metallic impurities that are introduced in the material during the harsh conditions of graphite oxidation and can remain adsorbed during the subsequent post-reaction treatments and reductions. Particularly, when following the Hummers or related chemical oxidation methods to convert graphite into graphite oxide the presence of manganese and other metal impurities can be introduced in the resulting material.[12, 13] For example, EPR and/or NMR techniques allowed detection of isolated trace amounts of paramagnetic Mn^{2+} ions in GO or rGO sample obtained by Hummers method.[111-113] These impurities frequently in the range of hundreds of ppm or even larger depending on the extent of the purification of the material, can later be responsible for the catalytic activity inducing to some errors, particularly when claiming defective graphenes as metal-free catalysts. A good practice when preparing GO is to perform exhaustive consecutive washings to remove as much as possible the metal impurities. Unfortunately, frequently is not possible to remove completely these metal impurities.

In this regard, a catalytic test for those reactions claimed as promoted by graphene as metal-free catalyst is to add on purpose increasing amounts of metals, such as manganese, in the range of concentrations present on graphene and determine the influence of this contamination on the performance of contaminated graphene (Figure 11).[114] It is even possible a quantitative estimation of the catalytic activity of the material in the absence of metal from the extrapolation to a hypothetical zero-metal content of the plot of initial reaction rate versus the concentration of the metal in the ppm range.[114, 115] As representative examples of the possible influence of metals, particularly Mn, but also Fe and Cu, on the catalytic activity, it has been determined that rGO has intrinsic activity as metal-free Fenton catalyst for the phenol degradation by plotting the initial reaction rate of phenol disappearance of a series of experiments with graphenes in where manganese was purposely added in the ppm range (Figure 11).[114, 115]

In contrast to the relatively minor influence of Mn^{2+} ions in the catalytic activity of rGO for the Fenton degradation of phenol, Pumera and co-workers have concluded in a series of papers that a large proportion of the claimed electrocatalytic activity of graphene materials is due to the presence of metal impurities typically present also in the ppm range.[90, 105, 106, 116, 117] The main electrocatalytic reactions in which the influence of metal impurities on graphene has been demonstrated are the oxygen reduction reaction[105, 116] and the hydrogen evolution reaction.[118] Starting from ultrapure-certified graphite as starting material a large variety of metal impurities, determined by neutron activation analysis or ICP-OES, was introduced in rGO.[117] The oxidation and reduction methods employed in rGO preparation determines the nature and proportion of the metal impurities present finally in the material (Scheme 1). The oxidizing agent employed in the Hummers method is $KMnO_4$, while Staudenmaier and Hofmann methods employ $KClO_3$.

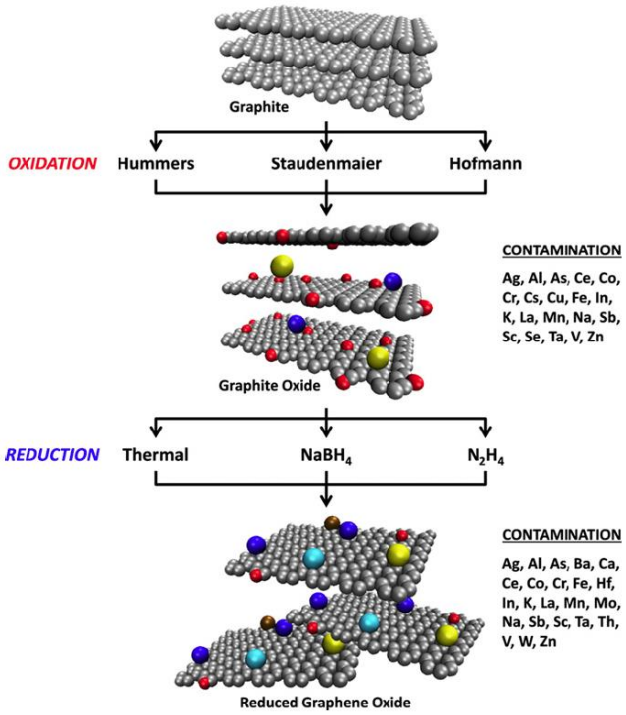

Figure 11. a) Conditions of the Fenton degradation of phenol by H_2O_2 using defective graphenes as catalyst, b) influence of the presence of Mn^{2+} ions as purposely added impurity on the catalytic activity of rGO for the heterogeneous Fenton reaction.[114, 115]

In terms of metal impurities, the most salient feature of Hummer's oxidation is the presence of a large amount of Mn (2.290 ppm) in the resulting GO due to the use of an excess of $KMnO_4$ as oxidant. [117] Importantly, other unexpected metallic and metalloid elements (As, Co, Cr, Cs, Cu, Fe, Sb and Sc) were also present in various concentrations in the GO sample, and supposed to be present in the reagents employed.[117] Chemical analysis showed in this study that the reduction of GO by

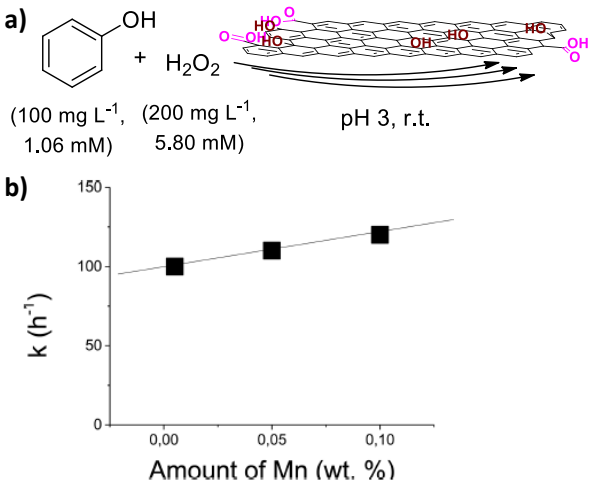

Scheme 1. Common synthetic methods employed for the preparation of rGO samples using graphite as a starting material, which ultimately lead to various levels of contamination from metal impurities present in the chemical agents used. Gray and red spheres represent carbon and oxygen atoms, respectively, and other colors represent metallic impurities.[117]

thermal or chemical methods results in an increase in the concentration of Fe impurities. On one hand, for the oxygen reduction reaction it was demonstrated that the presence of Mn in the rGO samples shifts the onset potential to more positive values respect to the use of noncatalytic bare glassy carbon electrode (-265 mV). On the other hand, the presence of Fe impurities in the rGO was correlated with the observed shift to more positive values of the potential for cumene hydroperoxide reduction. The rGO samples prepared by the Hofmann or Staudenmaier methods also present 15 or 11 different metal impurities, respectively. The smaller number of impurities and their lower concentration in the rGO samples obtained by the Staudenmaier method respect to those obtained by the Hofmann procedure was attributed to the use of fuming nitric acid as corrosive reagent. Although Mn trace levels were lower than 97 ppm in the samples used as electrodes, the presence of Ni in the rGO sample was found to have a correlation with the onset potentials for the electrocatalytic oxidation of hydrazine.[117] Overall the rigorous study correlating metal impurities and electrocatalytic activity of the graphene samples shows conclusively that the presence of these metals at ppm levels exert a strong influence on electrocatalytic measurements.

In another work, it was similarly shown that iron impurities present in graphene materials participate as active sites in the observed peroxidase-like catalytic activity of this sample (Figure 12a).[74] This study determined that graphene obtained from exfoliation of graphite using NMP as solvent and low-power sonication, low-oxygen graphene (14 wt%) obtained using $KMnO_4/H_2O_2$ as oxidant and GO from Hummers method exhibited catalytic activity towards the peroxidase-like reaction. The activity in these graphene materials was, however, attributed to the presence of iron determined by EDX measurements (Figure 12b). This hypothesis was further confirmed by performing selective quenching experiments using fluoride ions and observing that the catalytic activity is almost suppressed. The ability of fluoride ions to axially coordinate to the iron centers blocking their interaction with H_2O_2 is well established in this area. In additional type of catalytic experiments, the ability of a graphene sample to which iron was purposely added was compared with the catalytic activity without Fe addition providing further evidence about the role of iron on the observed catalytic activity of graphenes in the peroxidase-like H_2O_2 decomposition (Figure 12c). Similarly, the possible role of Mn^{2+} ions on the catalytic activity of the materials prepared by using $KMnO_4$ as oxidant towards the peroxidase reaction should have also been addressed to assess what influence can be expected from these impurities on the catalytic activity of graphenes.

In contradiction with the general assumption of the high quality and purity of graphene obtained by CVD, it has been reported that metal impurities such as Cu or Ni can be present in the material.[75] These metal impurities include not only Cu or Ni metals employed as catalysts in the CVD method, but also Fe derived from the use of iron-based etching solutions (i.e. $FeCl_3$ or $Fe(NO_3)_3$) to remove Cu or Ni from the graphene film (Figure 13).[75] Thus, it is highly important to take into account the possible influence of these metal impurities on the resulting catalytic activity of the CVD graphene. In this line, as previously commented, Pumera and co-workers have reported comprehensive analytical data showing the favorable role of these metal impurities present in CVD graphene on its resulting electrocatalytic activity.[75, 90]

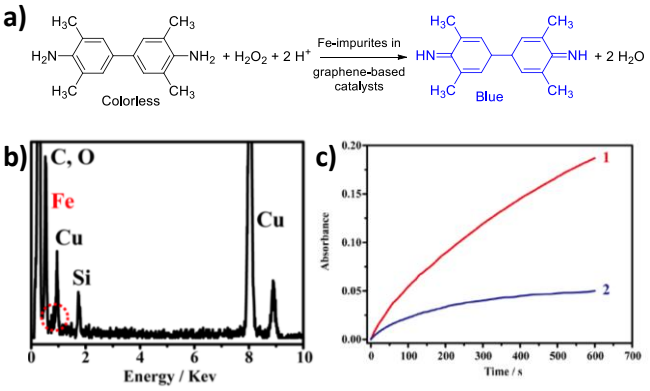

Figure 12. a) Peroxidase-like activity of graphenes to activate H_2O_2 using 3,3',5,5'-tetramethylbenzidine (TMB) as probe; b) EDX profile of low-oxygen content graphene; c) Time-dependent absorbance changes at 652 nm of peroxidase-like activation of TMB catalyzed by low-oxygen graphene (1) before and (2) after the addition fluoride ions.[74]

In another interesting work, Balasubramanian and co-workers have demonstrated that copper traces remaining in CVD synthesized graphene due to the incomplete removal of this metal may result in an important enhancement of both the electrochemical activity and electronic-transport properties of graphene (Figure 13).[76] One of the procedures for copper etching from graphene employs a metal-free

solution of HCl with H_2O_2 that allows the removal of more than 90 % of copper from graphene as revealed by time-of-flight secondary ion mass spectrometry. The selection of HCl for the etching procedure is based on the higher stability of graphene towards this acid compared to analogous acid solutions of H_2SO_4 or HNO_3.[119] Based on AFM and Raman spectroscopy, this study concluded that the etching procedure does not alter the physico-chemical properties of graphene, even though some residual Cu is still detectable on the sample.[76] These findings highlight the importance of graphene purification from metal impurities for its use in catalysis and electrocatalysis as well as for the development of electronic devices where the electronic-transport properties play a key role on the overall process efficiency.

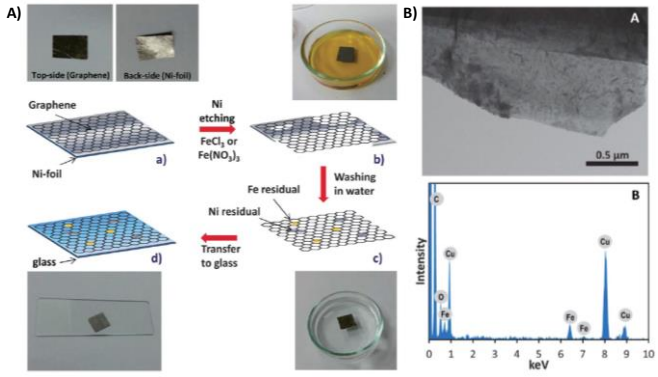

Figure 13. A Schematic of the adopted transfer process of graphene films after CVD preparation. (a) CVD-multilayer graphene sample grown on Ni foil polished at one side to remove the graphene film on that face to facilitate the removal of the Ni foil. (b) Etching of the Ni metal using $FeCl_3$ or $Fe(NO_3)_3$ solution. (c) After completing dissolution of Ni, the graphene film is suspended in distilled water. This washing step is repeated several times to remove the excess Fe employed in etching solution. (d) The graphene film is transferred to a clean glass slide. The photographs show the visual appearance of the sample in each step of the process. Despite the careful etching and washing steps, contamination from remaining Ni and Fe metals was observed (corresponding to as grey and yellow dots, respectively). B (A) STEM images of CVD graphene films loaded onto C/Cu TEM grids after the washing procedures showing sheets with dark spots. (B) Energy dispersive (EDX) analysis confirming the presence of Fe metal. Note that Cu signals were derived from the C/Cu TEM grid used for the analysis.[76]

Overall the above studies have shown the importance of providing exhaustive analytical data of graphene samples, particularly when claiming the use of these materials as metal-free catalyst or electrodes. When metals are detected attempts to freed the graphene samples from these impurities by applying physical or chemical methods should be made.[103](ref Hou) Acids typically can dissolve the metal ions...[103]

5.2. Presence of functional groups

5.2.1. Oxygen functional groups

One strategy for the production of high quality graphene is the direct exfoliation of graphite in different solvents assisted by sonication.[120] This strategy is the preferred one to obtain graphene materials with low density of defects and, thus, maintaining a large degree of the mechanical, optical and electronic properties expected in ideal graphene required for some applications in photo- and electrocatalysis. Common solvents[120] include *o*-dichlorobenzene and N-methyl-2-pyrrolidone (NMP), although the use of viscous solvents such as ionic liquids has been also reported.[121, 122] However, it has been found that ultrasonication can induce the generation of oxygenated species and other defects onto the resulting exfoliated graphene sheets.[77] Graphite flakes exfoliation to graphene in o-dichlorobenzene of NMP increases along sonication time and power. The highest concentration of exfoliated graphene (43.4 µg/mL) was achieved in this study when using a sonication power of 40 W for 60 min and *o*-dichlorobenzene as solvent.[77] Under these conditions, elemental analysis revealed an increase of the surface atomic percentage of oxygen from graphite to exfoliated graphene from 1.8 to 11 %, respectively. The presence of air during the sonication was proposed as the main source of oxygen introduced in the exfoliation process. Carboxylic and ether/epoxide groups were according to XPS (Figure 14) and ATR-IR spectroscopy the functional groups generated in the exfoliation. The introduction of defects in the exfoliated graphene was also characterized by Raman spectroscopy, observing the appearance of a new D band at 1350 cm^{-1}. These characterization data highlight that direct graphite exfoliation in a solvent by ultrasonication does not necessary produces defect-free graphene. This finding could be particularly important when using this type of material as carbocatalyst, where the presence of oxygenated functional groups may have a role as active sites.

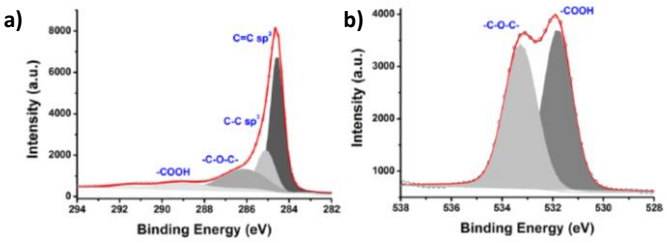

Figure 14. High-resolution XPS C1s (a) and O1s (b) peaks and their best deconvolution to individual components determined for graphene obtained from graphite exfoliation by ultrasonication in *o*-dichlorobenzene.[77]

Heteroatom doping of graphene materials is an important strategy to modify the electronic properties of graphenes and, therefore, their resulting photo-, electro- and catalytic activity.[123] Common doping or co-doping heteroatoms are N,

P, S, B and O that can be located on the basal plane or at the edges of graphene sheet.

The different methods reported for heteroatom doping can be classified as in situ (CVD, biopolymer pyrolysis, ball milling and bottom-up synthesis) or post-treatment (wet chemical methods, thermal annealing of GO with heteroatom precursors, plasma, arch discharge) methods. Preparation of doped graphenes and their main properties of these materials have been sufficiently reviewed.[73, 123, 124] Among them, thermal annealing of GO with a compound containing the required heteroatom has been widely used for the preparation of doped graphenes with enhanced catalytic activity.

A novel approach for the preparation of heteroatom-doped graphenes is based on the use of natural polysaccharides such as alginate,[125, 126] chitosan[127-129] or carrageenan[130] modified or not with additional heteroatoms forming the corresponding inorganic esters such as borate or phosphate.[131-133] Scheme 2 illustrates this preparation procedure of doped defective graphenes.[128] Frequently, following these preparation procedures the resulting defective graphenes present the wanted heteroatom doping, together with some residual oxygen functional groups. For example, even though GO thermal reduction or biopolymer pyrolysis are carried out at temperatures higher than 900 ºC, a residual oxygen content that can be as high as 10 wt% is frequently observed. However, the possibility that the residual oxygen content is playing a role as active site has been commonly neglected and the catalytic activity of the doped graphene attributed exclusively to the heteroatom other than oxygen. For this reason, more efforts should be done to confirm or exclude the influence that the presence of residual oxygen content exerts on the resulting catalytic activity of doped graphenes.

In other examples, GO has been reduced to rGO by using L-ascorbic acid (Scheme 3).[134] The obtained rGO has a good dispersability in water at room temperature for several days. This fact was attributed to the functionalization of the rGO sheet by oxalic and guluronic acids formed during the chemical reduction from ascorbic acid. This association of rGO with byproducts of the chemical reduction prevents the stacking of the rGO sheets.[134-136]

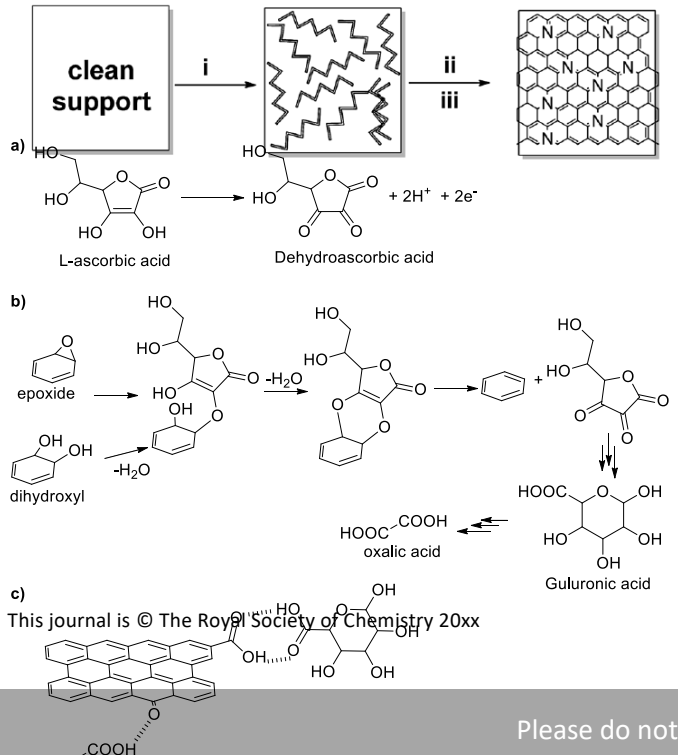

Scheme 2. Illustration of the preparation procedure of N-doped graphene films by (i) spin coating of chitosan, followed by (ii) annealing at 200 ºC for 2 h and (iii) calcination at temperatures between 600 and 1200 ºC.[128]

Scheme 3. a) L-Ascorbic oxidation to dehydroascorbic acid; b) Proposed mechanisms for the reduction of epoxide and dihydroxyl groups with L-ascorbic acid; c) Illustration of rGO association with oxalic and guluronic acid that improves rGO dispersability in aqueous suspensions.

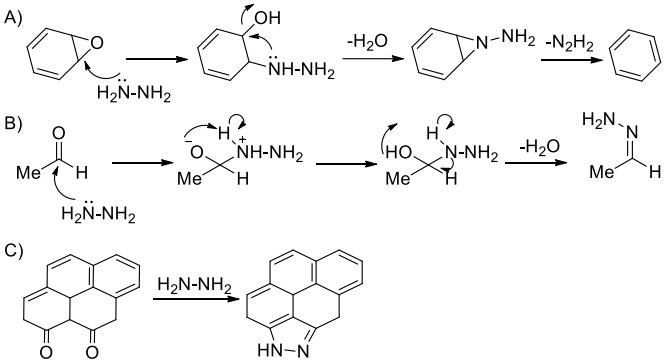

In other cases, hydroquinone is employed as reducing agent for the transformation of GO to rGO. In this case, exhaustive washings are needed to remove possible excess of hydroquinone or its oxidized product p-benzoquinone that could become active sites for some reactions. Recently it was been proposed that the hydroquinone/p-benzoquinone pair can act as redox centers for the activation of H_2O_2 [114, 137] or peroxymonosulfate oxidants.[69]

5.2.2. Nitrogen functional groups

rGO can be obtained from GO[63, 135] by using hydrazine as reducing agent.[50, 138, 139]. Elemental analysis clearly reveals the reduction of the oxygen content in the transformation from GO to rGO by chemical reduction with hydrazine. In addition, these elemental analysis data frequently indicate that the reduction process is also accompanied by the incorporation of some nitrogen from the reducing agent presumably in the form of hydrazones, amines, aziridines or other related structures.[50, 60, 63]. Hydrazine can react with anhydrides and lactones to form hydrazides and with quinones to form hydrazones.[140] Incomplete reduction of epoxy groups with hydrazine can afford hydrazine alcohols that could be further converted to other nitrogenated functional groups attached to rGO (Scheme 4).[63, 141-143]

Due to the toxicity of hydrazine[144-146] some studies have focused in developing greener reducing procedures. Alternative reducing agents for the production of rGO include amino acids such as L-alanine,[147] glycine,[148] L-lysine[149] and 2,4-dihydroxylphenyl alanine,[150] peptides such as glycylglycine,[78] proteins such as bovine serum albumin[151] or other nitrogen-containing natural products.[135] Similarly to the use of

Scheme 4. Proposed mechanisms[50, 152-154] for the reduction of GO by hydrazine: A) epoxide groups, B) carbonylic groups and C) Formation of the pyrazole ring from vicinal diketones.

hydrazine as GO reducing agent, it is likely that also these organic nitrogenated reductants cause also nitrogen functionalization in the resulting rGO.[135] Although this possibility has not always been considered, it is likely that N functional groups introduced in the GO reduction could be responsible for some of the physico-chemical properties of the resulting rGO samples, as well as their catalytic activity. In general, the use amino acids leads to rGO samples that disperse very well in water, a fact that can be attributed to the presence of the carboxylate groups of the reducing agent, if somehow it becomes attached. Scheme 5 illustrates some steps proposed to occur in the reduction process of GO to rGO using L-alanine.[147]

In one example, it has been demonstrated that the reduction of GO to rGO using glycylglycine takes places simultaneously with the incorporation of nitrogen in rGO.[78] In particular, thermogravimetric analysis, FT-IR spectroscopy and XPS measurements of the resulting rGO revealed the presence of imine and positively charged N atoms, while the presence of primary or secondary amine groups (–NH_2 or NH) was not detected. It was proposed that amine groups, even those attached to rGO, should become oxidized during the reducing process.[78]

In addition to the previous sections, a vast number of substances have been described to be able to reduce GO to rGO including inorganic reducing agents such as $NaBH_4$,[60] aluminum powder,[155] iron powder[156] etc or organics compounds bearing amino groups like in the case of benzylamine,[157] ethylenediamine,[158] hydroxylamine,[159] *p*-phenylenediamine,[160] pyrrole,[161] melatonin[162, 163] etc. or hydroxyl groups[138] such as reducing sugars[146], polyphenolic compounds,[164-166] glucose[165] and even bacteria[167]. The

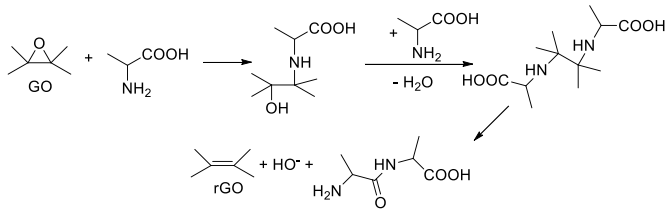

Scheme 5. Possible mechanism of reduction of GO to rGO with alanine. Note that some nitrogenated intermediates could still be present in the final complex structure of rGO.

resulting rGO material, even though is vigorously washed can be functionalized in some extent with the reducing agent or its oxidized version and this could affect to the observed catalytic activity. Exhaustive analytical data should be provided for these graphene samples and the possible role of those impurities in the observed catalytic activity addressed in detail.

5.2.3. Sulfur functional groups

GO preparation from graphite typically employs harsh conditions with the presence of oxidants in sulfuric medium. In a series of papers some unexpected catalytic activity of GO for acid-catalyzed reactions such as acetalization of aldehydes[79] and epoxide ring opening[80] were observed and the acid activity attributed to the presence of residual sulfate and sulfonic groups (Scheme 6). The difference between these two functional groups is the bond through which the S atom remains attached to the rGO sheet, either C-O (sulfate) or C-S (sulfonate) bonds. C-OSO_3H is more labile and easier to be hydrolyzed and lost during the reaction.

Analogously the ability of rGO for cellulose hydrolysis and glucose transformation have been found to be attributable to the presence of sulfonic groups attached to rGO as impurities.[168] In this regard, a good practice is to provide elemental analysis of the graphene samples under study to determine the presence of sulfur, particularly when studying GO or rGO as acid catalysts. A way to support the possible role of hydrogen sulfate groups on the catalyst is to treat the graphene suspension in alcoholic solution that should remove part of those groups by methanolysis.

Similarly to the case of α-aminoacids, L-cysteine has been used as reducing agent for the preparation of rGO from GO.[169] In this case, however, the thiol groups can also be involved in the chemical reduction, resulting in their oxidation to disulfides as byproducts. A possible reaction mechanism is indicated in Scheme 7. According to this Scheme, there are several possible ways in which cysteine can become also attached to the graphene sheet of the resulting rGO and could introduce functional groups with some catalytic activity.

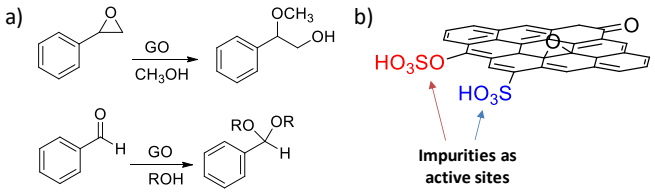

Scheme 6. a) Ring opening epoxide and acetalization of aldehydes using GO as catalyst; b) Illustration of sulfate or sulfonic acid groups that could be present in GO acting as active sites.

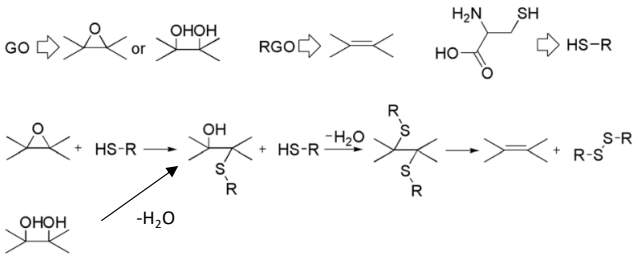

Scheme 7. Proposed pathways for the reduction of GO to rGO by using L-cysteine.[169]

5.3. Amorphous carbon as impurities

The presence of amorphous carbon impurities in graphene has been reported as responsible for the observed electrocatalytic activity towards NADH, hydroquinone and

acetaminophen.[81] In previous reports,[170] the presence of active carbonaceous impurities in CNTs for the electrocatalysis of compounds including azo compounds,[171] organic hydrazines,[172] some amino acids,[173] NADH,[170, 174] hydroquinone[171] and acetaminophen[175] has been reported.

Analogously, Loh and co-workers have observed by transmission electron microscopy that the deep chemical Hummers oxidation of graphite can result in the formation of some debris constituted by amorphous carbon containing large density of carboxylic acid groups.[82] These amorphous carbon debris are mostly located at holes on the GO. Removal of these amorphous carbon particles can be performed by basic washing of the raw GO resulting from Hummers oxidation. Subsequently, the GO purified of the amorphous particles is submitted to acid washings to recover carboxylic acid groups present on GO. It was found that the catalytic activity of base and acid treated GO for the aerobic oxidation of benzyl amines is much higher than that of the pristine GO, leading to the conclusion that the amorphous carbon particles play a detrimental role on the catalytic activity of GO. According to this study, a good practice should be to determine the absence of amorphous carbon particles on the graphene samples and proceed to their removal to evaluate the intrinsic catalytic activity of GO samples.

6. Concluding remarks

It can be anticipated that the search for sustainable catalysts based on abundant elements will continue in the next years and that graphenes and related materials will consolidate as one of the most versatile platform for developing such catalysts. This research on graphenes catalysts should bridge the gap between organocatalysis and catalysis by metals and should clarify the nature of the active sites that can promote different types of general organic reactions and how to engineer these sites on the graphene sheet.

As the field progresses, the initial, preliminary issues that are discussed in the present perspective should be clarified and a general consensus on the scientific community should be reached, probably with the appearance of new concepts of material design derived from graphenes and the broaden and more flexible interpretation of some features characteristic of ideal graphene. Issues such as considering or not graphene materials with a considerable density of defects or having a large proportion of heteroatoms or having multilayer configuration will be evolve, leading to a wide consensus by the scientific community practicing the field. Similarly, it is expected that the role of impurities, either metallic or carbonaceous, on the catalytic activity will be addressed for many different reaction types, laying out a better defined panorama of what general reaction types can or cannot be catalyzed by graphenes, what are the wanted centers for these transformations and how to avoid undesirable, adventitious sites that are detrimental for the selectivity. Our hope in this perspective is to contribute to a general discussion around some of the open issues in the field.

Conflicts of interest

There are no conflicts to declare.

Acknowledgements

Financial support by the Spanish Ministry of Economy and Competitiveness (Severo Ochoa and CTQ2014-53292-R is gratefully acknowledged. Generalidad Valenciana is also thanked for funding (Prometeo 2013/014). SN thanks financial support by the Fundación Ramón Areces (XVIII Concurso Nacional para la Adjudicación de Ayudas a la Investigación en Ciencias de la Vida y de la Materia, 2016).

Notes and references

1. S. Cao, F. F. Tao, Y. Tang, Y. Li and J. Yu, *Chem. Soc. Rev.*, 2016, **45**, 4747-4765
2. R. Chinchilla and C. Nájera, *Chem. Rev.*, 2007, **107**, 874-922.
3. J. Pritchard, G. A. Filonenko, R. Van Putten, E. J. M. Hensen and E. A. Pidko, 2015, **44**, 3808-3833.
4. M. Stratakis and H. Garcia, *Chem. Rev.* , 2012, **112**, 4469-4506.
5. L. Yang and H. Huang, *Chem. Rev.*, 2015, **115**, 3468-3517.
6. I. Bauer and H.-J. Knölker, *Chem. Rev.*, 2015, **115**, 3170-3387.
7. M. B. Gawande, A. Goswami, F.-X. Felpin, T. Asefa, X. Huang, R. Silva, X. Zou, R. Zboril and R. S. Varma, 2016, **116**, 3722-3811
8. M.-M. Titirici, R. J. White, N. Brun, V. L. Budarin, D. S. Su, F. del Monte, J. H. Clark and M. J. MacLachlan, *Chem. Soc. Rev.*, 2015, **44**, 250-290.
9. C. K. Chua and M. Pumera, *Chem. Eur. J.*, 2015, **21**, 12550-12562.
10. D. R. Dreyer and C. W. Bielawski, *Chem. Sci.*, 2011, **2**, 1233-1240.
11. D. R. Dreyer, A. D. Todd and C. W. Bielawski, *Chem. Soc. Rev.*, 2014, **43**, 5288-5301.
12. S. Navalon, A. Dhakshinamoorthy, M. Alvaro, M. Antonietti and H. García, *Chem. Soc. Rev.*, 2017, **46**, 4501-4529
13. S. Navalon, A. Dhakshinamoorthy, M. Alvaro and H. Garcia, *Chem. Rev.*, 2014, **114**, 6179-6212.
14. D. S. Su, S. Perathoner and G. Centi, *Chem. Rev.*, 2013, **113**, 5782-5816.
15. D. S. Su, G. Wen, S. Wu, F. Peng and R. Schlögl, *Angew. Chem. Int. Ed.*, 2017, **56**, 936-964.
16. P. Tang, G. Hu, M. Li and D. Ma, *ACS Catal.*, 2016, **6**, 6948-6958.
17. S. Navalon, A. Dhakshinamoorthy, M. Alvaro and H. Garcia, *Coord. Chem. Rev*, 2016, **312**, 99-148.
18. C. K. Chua and M. Pumera, *Chem. soc. Rev.*, 2013, **42**, 3222-3233.
19. V. Georgakilas, M. Otyepka, A. B. Bourlinos, V. Chandra, N. Kim, K. C. Kemp, P. Hobza, R. Zboril and K. S. Kim, *Chem. Rev.*, 2012, **112**, 6156-6214.
20. X. Huang, X. Qi, F. Boey and H. Zhang, *Chem. Soc. Rev.*, 2012, **41**, 666-686.

21. C. N. R. Rao, Sood, A.K., Subrahmanyam, K.S., Govindaraj, A., *Angew. Chem. Int. Ed.*, 2009, **48**, 7752-7777.
22. C. Soldano, A. Mahmood and E. Dujardin, *Carbon*, 2010, **48**, 2127-2150.
23. J. Duan, S. Chen, M. Jaroniec and S. Z. Qiao, *ACS Catal.*, 2015, **5**, 5207−5234.
24. J. Li, Z. Zhao, Y. Ma and Y. Qu, *ChemCatChem*, 2017, **9**, 1554 - 1568.
25. S. Navalón, J. R. Herance, M. lvaro and H. García, *Chem. Eur. J.*, 2017, **23**, 15244-15275.
26. X. Li, J. Yu, S. Wageh, A. A. Al-Ghamdi and J. Xie, *Small*, 2016, **48**, 6640-6696.
27. J. Low, J. Yu, M. Jaroniec, S. Wageh and A. A. Al-Ghamdi, *Adv. Mater.*, 2017 **29**, 1601694.
28. D. Haag and H. H. Kung, *Top. Catal.*, 2014, **57**, 762-773.
29. Editorial, *Carbon*, 2013, **65**, 1-6.
30. A. K. Geim and K. S. Novoselov, *Natur. Mater.*, 2007, **6**, 183-191.
31. Y. Li, H. Wang, L. Xie, Y. Liang, G. Hong and H. Dai, *J. Am. Chem. Soc.*, 2011, **133**, 7296-7299.
32. P. Wick, A. E. Louw-Gaume, M. Kucki, Harald F. Krug, K. Kostas Kostarelos, B. Bengt Fadeel, K. A. Kenneth A. Dawson, A. Salvati, E. Vázquez, L. Ballerini, M. Tretiach, F. Benfenati, E. Flahaut, L. Gauthier, M. Prato and A. Bianco, *Angew. Chem. Int. Ed.*, 2014, **53**, 7714 - 7718.
33. D. Mateo, J. Albero and H. García, *Appl. Catal. B. Environ.*, 2018, **224**, 563-571.
34. M. Oa, Q. Zhonga, S. Zhanga, H. Niea, Z. Lva and W. Caia, *Appl. Catal. B. Environ.*, 2016, **193**, 160-169.
35. A. Primo, F. Neatu, M. Florea, V. Parvulescu and H. Garcia, *Nat. Commun.*, 2014, **5**, 5291.
36. V. Chabot, D. Higgins, A. Yu, X. Xiao, Z. Chena and J. Zhang, *Energy Environ. Sci.*, 2017, **7**, 1564-1596.
37. S. Chowdhury and R. Balasubramanian, *Prog. Mater. Sci.*, 2017, **90**, 224-275.
38. S. Shen, Q. Fang and B. Chen, *Environ. Sci. Technol.*, 2015, **49**, 67-84.
39. W. Jiang, H. Wang, Z. Xu, N. Li, C. Chen, C. Li, J. Li, H. Lv, L. Kuang and X. Tian, *Chem. Eng. J. (https://doi.org/10.1016/j.cej.2017.11.020)*, 2018.
40. X. Cao, Z. Yin and H. Zhang, *Energy Environ. Sci.*, 2014, **7**, 1850-1865.
41. Y. Huang, J. Liang and Y. Chen, *Small*, 2012, **8**, 1805-1834.
42. Y. Zhu, S. Murali, M. D. Stoller, K. J. Ganesh, W. Cai, P. J. Ferreira, A. Pirkle, R. M. Wallace, K. A. Cychosz, M. Thommes, D. Su, E. A. Stach and R. S. Ruoff, *Science*, 2011, **332**, 1537-1541.
43. S. Gadipelli and Z. X. Guo, *Prog. Mater. Sci.*, 2015, **69**, 1-60.
44. J. Pérez-Ramírez, C. H. Christensen, K. Egeblad, C. H. Christensen and J. C. Groen, *Chem. Soc. Rev.*, 2008, **37**, 2530-2542.
45. Y. Tao, H. Kanoh, L. Abrams and K. Kaneko, *Chem. Rev.*, 2006, **106**, 896-910.
46. H. Furukawa, K. E. Cordova, M. O'Keeffe and O. M. Yaghi, *Science*, 2013, **341**, 1230444.
47. Y. Wan and D. Zhao, *Chem. Rev.*, 2007, **107**, 2821-2860
48. D. W. Lewis, D. J. Willock, C. R. A. Catlow, J. M. Thomas and G. J. Hutchings, *Nature*, 1996, **382**, 604-607.
49. X. PengTao, Y. JiXiang, W. KeSai, Z. Zhen and S. PanWen, *Chin. Sci. Bull.*, 2012, **57**, 2948-2955.
50. S. Stankovich, D. A. Dikin, R. D. Piner, K. A. Kohlhaas, A. Kleinhammes, Y. Jia, Y. Wu, S. T. Nguyen and R. S. Ruoff, *Carbon*, 2007, **45**, 1558-1565.
51. J. Wang and S. Kaskel, *J. Mater. Chem.*, 2012, **22**, 23710-23725
52. R. Kumar, V. M. Suresh, T. K. Maji and C. N. R. Rao, *Chem. Commun.*, 2014, **50**, 2015-2017.
53. L. Zhang, F. Zhang, X. Yang, G. Long, Y. Wu, T. Zhang, K. Leng, Y. Huang, Y. Ma, A. Yu and Y. Chen, *Sci. Rep.*, 2012, **3**, 1408.
54. M. J. McAllister, J. L. Li, D. H. Adamson, H. C. Schniepp, A. A. Abdala, J. Liu, M. Herrera-Alonso, D. L. Milius, R. Car, R. K. Prud ' homme and I. A. Aksay, *Chem. Mater.*, 2007, **19**, 4396 − 4404.
55. P. Montes-Navajas, N. G. Asenjo, R. Santamaría, R. Menéndez, A. Corma and H. García, *Langmuir*, 2013, **29**, 13443–13448.
56. R. R. Nair, P. Blake, A. N. Grigorenko, K. S. Novoselov, T. J. Booth, T. Stauber, N. M. R. Peres and A. K. Geim, *Science*, 2008, **320**, 1308.
57. R. John, A. Ashokreddy, C. Vijayan and T. Pradeep, *Nanotechnology*, 2011, **22**, 165701
58. C. H. An Wonga, Z. ek Soferb, M. Kubešovác, J. Kucerac, S. Mat ejkovád and M. Pumera, *PNAS*, 2014, **111**, 13774–13779.
59. S. Park, J. An, J. R. Potts, A. Velamakanni, S. Murali and R. S. Ruoff, *Carbon*, 2011, **49**, 3019-3023.
60. H.-J. Shin, K. K. Kim, A. Benayad, S.-M. Yoon, H. K. Park, I.-S. Jung, M. H. Jin, H.-K. Jeong, J. M. Kim, J.-Y. Choi and Y. H. Lee, *Adv. Funct. Mater.*, 2009, **19**, 1987-1992.
61. W. Bragg, *Nature*, 1925, **114**, 862-865.
62. K. Muthoosamy, R. G. Bai, I. B. Abubakar, S. M. Sudheer, H. N. Lim, H.-N. Loh, N. M. Huang, C. H. Chia and S. Manickam, *International Journal of Nanomedicine*, 2015, **10**, 1505-1519.
63. D. R. Dreyer, S. Park, C. W. Bielawski and R. S. Ruoff, *Chem. Soc. Rev.*, 2010, **39**, 228-240.
64. A. Eftekhari and H. García, *Mater. Today Chem.*, 2017, **4**, 1-16.
65. L. Liu, M. Qing, Y. Wang and S. Chen, *J. Mater. Sci. Technol.*, 2015, **31**, 599-606.
66. F. Banhart, J. Kotakoski and A. V. Krasheninnikov, *ACS Nano*, 2011, **5**, 26-41.
67. A. Hashimoto, K. Suenaga, A. Gloter, K. Urita and S. Iijima, *Nature*, 2004, **430**, 870-873.
68. M. H. Al-Abboodi, F. N. Ajeel and A. M. Khudhair, *Physica E*, 2017, **88**, 1-5.
69. X. Duan, H. Sun, Z. Ao, L. Zhou, G. Wang and S. Wang, *Carbon*, 2016, **107**, 371-378.
70. J. Albero and H. Garcia, *J. Mol. Catal. A-Chem.*, 2017, **408**, 264–278.
71. J. Albero and H. Garcia, *J. Mol. Catal. A-Chem.*, 2015, **408**, 296-309.
72. S. Agnoli and M. Favaro, *J. Mater. Chem.*, 201, **4**, 5002-5025.
73. X.-K. Kong, C.-L. Chen and Q.-W. Chen, *Chem. Soc. Rev.*, 2014, **43**, 2841-2857.
74. Y. Dong, J. Li, L. Shi and Z. Guo, *ACS Appl. Mater. Interfaces*, 2015, **7**, 15403−15413.
75. A. Ambrosi and M. Pumera, *Nanoscale*, 2014, **6**, 472-476.

76. R. M. Iost, F. N. Crespilho, L. Zuccaro, H. K. Ki Yu, A. M. M. Wodtke, K. Kern and K. Balasubramanian, *ChemElectroChem*, 2014, **1**, 2070 - 2074.
77. T. Skaltsas, X. Ke, C. Bittencourt and N. Tagmatarchis, *J. Phys. Chem. C*, 2013, **117**, 23272−23278.
78. C. Zhang, M. Chen, X. Xu, L. Zhang, L. Zhang, F. Xia, X. Li, Y. Liu, W. Hu and J. Gao, *Nanotechnol.*, 2014, **25**, 135707.
79. A. Dhakshinamoorthy, M. Alvaro, M. Puche, V. Fornes and H. Garcia, *ChemCatChem*, 2012, **4**, 2026-2030.
80. A. Dhakshinamoorthy, M. Alvaro, P. Concepción, V. Fornés and H. Garcia, *Chem. Commun.*, 2012, **48**, 5443-5445.
81. L. Wang, A. Ambrosi and M. Pumera, *Chem. Asian J.*, 2013, **8**, 1200-1204.
82. C. Su, M. Acik, K. Takai, J. Lu, S. J. Hao, Y. Zheng, P. Wu, Q. Bao, T. Enoki, Y. J. Chabal and K. P. Loh, *Nat. Commun.*, 2012, **3**, 1298.
83. R. K. Arvela, N. E. Leadbeatr, M. S. Sangi, V. A. Williams, P. Granados and R. D. Singer, *J. Org. Chem.*, 2005, **70**, 161-168.
84. S. L. Buchwald and C. Bolm, *Angew. Chem. Int. Ed.*, 2009, **48**, 5586-5587.
85. P. F. Larsson, A. Correa, M. Carril, P. O. Norrby and C. Bolm, *Angew. Chem. Int. Ed.*, 2009, **48**, 5691-5693.
86. N. E. Leadbeater and M. Marco, *Angew. Chem. Int. Ed.*, 2003, **42**, 1407-1409.
87. M. Xue, G. Chen, H. Yang, Y. Zhu, D. Wang, J. He and T. Cao, *J. Am. Chem. Soc.*, 2012, **134**, 6536-6539.
88. F. M. Hu, T. Ma, H.-Q. Lin and J. E. Gubernatis, *Phys. Rev. B Condens. Matter.*, 2011, **84**, 075414.
89. A. V. Krasheninnikov and R. M. Nieminen, *Theor. Chem. Acc.*, 2011, **129**, 625-630.
90. A. Ambrosi, S. Y. Chee, B. Khezri, R. D. Webster, Z. Sofer and M. Pumera, *Angew. Chem. Int. Ed.*, 2012, **51**, 500 -503.
91. B. Sljuki, C. E. Banks and R. G. Compton, *Nano Lett.*, 2006, **6**, 1556-1558.
92. C. E. Banks, A. Crossley, C. Salter, S. J. Wilkins and R. G. Compton, *Angew. Chem. Int. Ed.*, 2006, **45**, 2533 -2537.
93. C. Batchelor-McAuley, G. G. Wildgoose, R. G. Compton, L. Shao and M. L. H. Green, *Sens. Actuators B Chem.*, 2008, **132**, 356-360.
94. X. Dai, G. G. Wildgoose and R. G. Compton, *Analyst*, 2006, **131**, 901-906.
95. A. Ambrosi and M. Pumera, *Chemistry* 2010, **16**, 1786-1792.
96. M. Pumera, A. Ambrosi and E. L. K. Chng, *Chem. Sci.*, 2012, **3**, 3347-3355.
97. K. Samant, V. S. Joshi, K. R. Patil and S. K. Haram, *Bull. Mater. Sci.*, 2014, **37**, 221-226.
98. K. Gong, D. F. Du, Z. Xia, M. Durstock and L. Dai, *Science*, 2009, **323**, 760-764.
99. W. Xiong, F. Du, Y. Liu, A. Perez, M. Supp, T. S. Ramakrishnan, L. Dai and L. Jiang, *J. Am. Chem. Soc.*, 2010, **132**, 15839-15841.
100. A. Morozan, P. Jegou, M. Pinault, S. Campidelli, B. Jousselme and S. Palacin, *ChemSusChem*, 2012, **5**, 647-651.
101. L. Feng, Y. Yan, Y. Chen and L. Wang, *Energy Environ. Sci.*, 2011, **4**, 1892-1899.
102. L. Yang, S. Jiang, Y. Zhao, L. Zhu, S. Chen, X. Wang, Q. Wu, J. Ma, Y. Ma and Z. Hu, *Angew. Chem., Int. Ed.*, 2011, **50**, 7132-7135.
103. P.-X. Hou, C. Liu and H.-M. Cheng, *Carbon*, 2008, **46**, 2003-2025.
104. M. Purmera, *Langmuir*, 2007, **23**, 6453-6458.
105. L. Wang, A. Ambrosi and M. Pumera, *Angew. Chem. Int. Ed.*, 2013, **52**, 13818 -13821.
106. A. Ambrosi, C. K. Chua, B. Khezri, Z. Sofer, R. D. Webster and M. Pumera, *PNAS*, 2012, **109**, 12899–12904.
107. L. Wang and M. Pumera, *Chem. Commun.*, 2014, **50**, 12662-12664.
108. T. Kolodiazhnyi and M. Pumera, *Small*, 2008, **4**, 1476–1484.
109. A. Nikitin, H. Ogasawara, D. Mann, R. Denecke, Z. Zhang, H. Dai, K. Cho and A. Nilsson, *Phys. Rev. Lett.*, 2005, **95**, 225507.
110. J. P. Smith, C. W. Foster, J. P. Metters, O. B. Sutcliffe and C. E. Banks, *Electroanalysis*, 2014, **26**, 2429 - 2433.
111. A. M. Panich, A. Shames, A. E. Aleksenskii and A. Dideikin, *Solid State Commun.*, 2012, **152**, 466-468.
112. B. S. Paratala, B. D. Jacobson, S. Kanakia, L. D. Francis and B. Sitharaman, *PLoS ONE*, 2012, **7**, e38185.
113. A. M. Panich, A. Shames and N. A. Sergeev, *Appl. Magn. Reson.*, 2013, **44**, 107-116.
114. J. C. Espinosa, S. Navalón, A. Primo, M. Moral, J. Fernández Sanz, M. Álvaro and H. García, *Chem. Eur. J.*, 2015, **21**, 11966–11971.
115. A. Primo, V. Parvulescu and H. Garcia, *J. Phys. Chem. Lett.*, 2017, **8**, 264-278.
116. L. Wang, C. K. Chua, B. Khezri, R. D. Webster and M. Pumera, *Electrochem. Commun.*, 2016, **62**, 17-20.
117. C. H. An Wong, Z. ek Sofer, M. Kubešová, J. Kucera, S. Matejková and M. Pumera, *PNAS*, 2014, **111**, 13774–13779.
118. W. Zhou, J. Jia, J. Lu, L. Yang, D. Hou, G. Li and S. Chen, *Nano Energ.*, 2016, **28**, 29-43.
119. S. M. Tan, A. Ambrosi, B. Khezri, R. D. Webster and M. Pumera, *Phys. Chem. Chem. Phys.*, 2014, **16**, 7058 -7065.
120. A. Ciesielski and P. Samorì, *Chem. Soc. Rev.*, 2014, **43**, 381-398.
121. P. Bhunia, E. Hwang, Y. Yoon, E. Lee, S. Seo and H. Lee, *Chem. Eur. J.*, 2012, **18**, 12207-12212.
122. S. Zhang, M. S. Miran, A. Ikoma, K. Dokko and M. Watanabe, *J. Am. Chem. Soc.*, 2014, **136**, 1690-1693.
123. X. Wang, G. Sun, P. Routh, D.-H. Kim, W. Huang and P. Chen, *Chem. Soc. Rev.*, 2014, **43**, 7067--7098.
124. Y. Xue, B. Wu, Q. Bao and Y. Liu, *Small*, 2014, **10**, 2975-2991.
125. P. Atienzar, A. Primo, C. Lavorato, R. Molinari and H. García, *Langmuir*, 2013, **29**, 6141-6146.
126. A. Primo, A. Forneli, A. Corma and H. García, *ChemSusChem*, 2012, **5**, 2207-2214.
127. C. Lavorato, A. Primo, R. Molinari and H. Garcia, *Chem. Eur. J.*, 2014, **20**, 187-194.
128. A. Primo, P. Atienzar, E. Sanchez, J. M. Delgado and H. García, *Chem. Commun.*, 2012, **48**, 9254-9256.
129. A. Primo, E. Sánchez, J. M. Delgado and H. García, *Carbon*, 2014, **68**, 777-783.
130. A. Dhakshinamoorthy, M. Latorre-Sanchez, A. M. Asiri, A. Primo and H. Garcia, *Catal. Commun.*, 2015, **65**, 10-13.

131. A. Dhakshinamoorthy, A. Primo, P. Concepcion, M. Alvaro and H. Garcia, *Chem. Eur. J.*, 2013, **19**, 7547-7554.
132. M. Latorre-Sánchez, A. Primo, P. Atienzar, A. Forneli and H. García, *Small*, 2015, **11**, 970-975.
133. M. Latorre-Sánchez, A. Primo and H. García, *Angew. Chem. Int. Ed.*, 2013, **52**, 11813-11816.
134. J. Zhang, H. Yang, G. Shen, P. Cheng, J. Zhang and S. Guo, *Chem. Commun.*, 2010, **46**, 1112-1114.
135. C. K. Chua and M. Pumera, *Chem. Soc. Rev.*, 2014, **43**, 291-312.
136. J. Gao, F. Liu, Y. Liu, N. Ma, Z. Wang and X. Zhang, *Chem. Mater.* , 2010, **22**, 2213-2218.
137. J. C. Espinosa, S. Navalón, M. Álvaro and H. García, *ChemCatChem*, 2016, **8**, 2642-2648.
138. D. R. Dreyer, S. Murali, Y. Zhu, R. S. Ruoff and C. W. Bielawski, *J. Mater. Chem.*, 2011, **21**, 3443-3447.
139. S. Park, J. An, I. Jung, R. D. Piner, S. An, X. Li, A. Velamakanni and R. S. Ruoff, *Nano Lett.* , 2009, **9**, 1593-1597.
140. R. Neidlein, T. V. Dao, A. Gieren, M. Kokkinidis, R. Wilckens and H. P. Geserich, *I. Chem Ber* 1982, **115**, 2898-2904.
141. Z. Zalan, L. Lazar and F. Fueloep, *Curr. Org. Chem.*, 2005, **9**, 357-376.
142. R. K. Mueller, D. Felix, J. Schreiber and A. Eschenmoser, *Helv. Chim. Acta*, 1970, **53**, 1479-1484.
143. P. M. Lahti, *Tetrahedron Lett.*, 1983, **24**, 2339-2342.
144. J. I. Paredes, S. Villar-Rodil, M. J. Ferández-Merino, L. Guardia, A. Martínez-Alonso and J. M. D. Tascón, *J. Mater. Chem.*, 2011, **21**, 298-306.
145. K. Ai, Y. Liu, L. Lu, X. Cheng and L. Huo, *J. Mater. Chem.* , 2011 **21**, 3365-3370.
146. C. Zhu, S. Guo, Y. Fang and S. Dong, *ACS Nano* 2010, **4**, 2429-2437.
147. J. Wang, E. C. Salihi and L. Šiller, *Mater. Sci. Eng.*, 2017, **72**, 1-6.
148. S. Bose, T. Kuila, A. K. Mishra, N. H. Kim and J. H. Lee, *J. Mater. Chem.* , 2012, **22**, 9696-9703.
149. J. Ma, X. Wang, Y. Liu, T. Wu, Y. Liu, Y. Guo, L. Ruqiang, X. Sun, F. Wu, C. Li and J. Gao, *J.Mater. Chem. A*, 2013, **1**, 2192-2201.
150. B. Adhikari and A. Banerjee, *Mater. Chem. Phys.*, 2013, **139**, 450-458.
151. J. Liu, S. Fu, B. Yuan, Y. Li and Z. Deng, *J. Am. Chem. Soc.*, 2010 **132**, 7279-7281.
152. X. Gao, J. Jang and S. Nagase, *J. Phys. Chem. C*, 2009, **114**, 832-842.
153. M. C. Kim, G. S. Hwang and R. S. Ruoff, *J. Chem. Phys.*, 2009, **131**, 064704.
154. S. Park, Y. Hu, J. O. Hwang, E.-S. Lee, L. B. Casabianca, W. Cai, J. R. Potts, H.-W. Ha, S. Chen, J. Oh, S. O. Kim, Y.-H. Kim, Y. Ishii and R. S. Ruoff, *Nat. Commun.*, 2012, **3**, 638.
155. Z. Fan, K. Wang, T. Wei, J. Yan, L. Song and B. Shao, *Carbon* 2010, **48**, 1686-1689.
156. Z. Fan, K. Wang, T. Wei, J. Yan, T. Wei, L. Zhi, J. Feng, Y. Ren, L. Song and F. Wei, *ACS Nano*, 2011, 191-198.
157. S. Liu, J. Tian, L. Wang and X. Sun, *Carbon* 2011, **49**, 3158-3164.
158. J. Che, L. Shen and Y. Xiao, *J. Mater. Chem.*, 2010 1722-1727.
159. X. Zhou, J. Zhang, H. Wu, H. Yang, J. Zhang and S. Gou, *J. Phys. Chem. C* 2011, **115**, 11957-11961.
160. Y. Chen, X. Zhang, P. Yu and Y. Ma, *Chem. Commun.* , 2009, 4527-4529.
161. C. A. Amarnath, C. E. Hong, N. H. Kim, B. C. Ku, T. Kuila and J. H. Lee, *Carbon* 2011, **49**, 3497-3502.
162. A. Esfandiar, O. Akhavan and A. Irajizad, *J. Mater. Chem.* , 2011, **21**, 10907-10914.
163. O. Akhavan, E. Ghaderi and A. Esfandiar, *J. Phys. Chem. B*, 2011, **115**, 6279-6288.
164. Y. Lei, Z. Tang, R. Liao and B. Guo, *Green Chem.* , 2011, **13**, 1655-1658.
165. O. Akhavan, E. Ghaderi, S. Aghayee, Y. Fereydooni and A. Talebi, *J. Mater. Chem.* , 2012 **22**, 13773-13781.
166. Y. Wang, Z. Shi and J. Yin, *ACS Appl. Mater. Interfaces* 2011, **3**, 1127-1133.
167. O. Akhavan and E. Ghaderi, *Carbon*, 2010, **50** 1853-1860.
168. X. Zhao, J. Wang, C. Chen, Y. Huang, A. Wang and T. Zhang, *Chem. Commun.*, 2014, **50**, 3439--3442.
169. D. Chen, L. Li and L. Guo, *Nanotechnol.*, 2011, **22**, 325601.
170. M. C. Henstridge, L. Shao, G. G. Wildgoose, R. G. Compton, G. Tobias and M. L. H. Green, *Electroanalysis*, 2008, **20**, 498-506.
171. E. J. E. Stuart and M. Pumera, *Chem. Asian J.*, 2011, **6**, 804-807.
172. E. J. E. Stuart and M. Pumera, *Phys. Chem. Chem. Phys.*, 2011, **13**, 10818-10822.
173. E. J. E. Stuart and M. Pumera, *Chem. Eur. J.*, 2011, **17**, 5544-5548.
174. L. Y. Chen, Y. H. Tang, K. Wang, C. B. Liu and S. L. Luo, *Electrochem. Commun.*, 2011, **13**, 133-137.
175. L. Wang, A. Ambrosi and M. Pumera, *Electrochem. Commun.*, 2013, **26**, 71-73.

